SIN-CHN
SCIENTIFIC PRESS PTE.LTD.

*Molecular & Cellular Biomechanics* 2025, 22(1), 1129.
https://doi.org/10.62617/mcb1129

Article

# Mechanical characterization of intracellular drug transport based on optimization of chemical engineering principles

**Mingfan Cai**

School of Bioengineering, Wuhan Vocational and Technical College, Wuhan 430070, Hubei, China; mingfan1222@163.com

**CITATION**

Cai M. Mechanical characterization of intracellular drug transport based on optimization of chemical engineering principles. Molecular & Cellular Biomechanics. 2025; 22(1): 1129.
https://doi.org/10.62617/mcb1129

**ARTICLE INFO**

Received: 17 December 2024
Accepted: 8 January 2025
Available online: 15 January 2025



**Abstract:** At present, the measurement of cellular mechanical properties is divided into contact and non-contact, combined with the actual situation of the research in this paper, according to which the optical tweezers measurement technology in the non-contact type is adopted. Taking the measured value of cellular mechanical properties as the entry point of this research, the optimization method commonly used in chemical engineering principles was adopted, and the optimization model based on the separation of viscoelasticity parameters was set up by constantly changing the viscoelasticity parameters of intracellular transport of drugs and setting up certain criteria to optimize and obtain the viscoelasticity parameters that best represent the mechanical properties of intracellular transport of drug cells. The model was used to experimentally analyze the mechanical properties of intracellular drug transport. The deformation of drug cells when reaching the predetermined elastic force was small when transported with the optimized transport speed curve of parameter $\eta$, and the transport speed was the largest, while the deformation obtained with the transport speed curve of parameter $k_2$ was between the two, indicating that the optimized speed curve of viscoelasticity parameter can effectively reduce the mechanical damage of the drug cells in the process of transport.

**Keywords:** optical tweezers measurement technique; chemical engineering principle; optimization model; drug cells; transport mechanical properties

## 1. Introduction

With the development of science and technology, people's requirements for the therapeutic effects and means of disease treatment are increasing. The research in the field of drug carriers focuses on improving the bioavailability of drugs, prolonging the duration of drug action, realizing in vivo targeting of drugs and reducing toxic side effects [1–3]. At present, drug carriers still have problems such as high development cost, narrow scope of application, low drug loading rate and low clinical application rate [4,5]. How to effectively deliver macromolecular drugs into cells remains a great challenge.

There are two routes of entry of macromolecular drugs into target cells, one is based on membrane rupture to introduce the drug directly into the cell, this route allows rapid delivery of almost all drugs dispersed in solution [6,7]. The membrane rupture-based delivery pathway allows the drug to enter the cell by transiently disrupting the cell membrane and repairing the membrane to restore intracellular homeostasis [8,9]. This approach is stringent on the extent and duration of cell membrane disruption and requires chemical modification of the drug to prevent degradation [10,11]. The other is the delivery vector route, which is categorized into viral and non-viral vectors. Viral delivery vectors can overcome cell membrane barriers and efficiently deliver macromolecular drugs into cells [12–14]. Despite the

high delivery efficiency of viral vectors for drugs, the limited drug loading capacity, high production cost, uncontrolled viral release, limited viral tropism, and safety concerns regarding the integration of viral genes into the host genome have not been fully addressed [15–18]. In contrast, non-viral delivery vectors have received extensive attention from scholars due to their lower immunogenicity, unrestricted drug carrying capacity, high flexibility, simple synthesis, low cost and easy storage [19–21].

In this paper, drug cell samples were first prepared using specialized experimental apparatus, and before the measurement of the mechanical properties of drug cell transport based on optical tweezers technology began, the stiffness of the optical trap was calibrated, and a freely suspended microsphere was found and captured by observing the petri dish using a 60× oil immersion objective. To address errors introduced by differences in drug cell sizes, 10 of the compliant drug cells in each sample were randomly selected for measurement. Subsequently, the conformational data of the cells after actual deformation were obtained directly from the experimental data based on the optical tweezers technique, and an objective function was defined to characterize the difference between the deformed cell conformations and the deformed cell conformations obtained through the experiments, and certain discriminative criteria were set up. The viscoelasticity parameters that best represent the mechanical properties of drug intracellular transport cells are optimized, and the construction of the optimization model of drug cell mechanical properties is completed. With the help of this model, the mechanical properties of drug intracellular transport were experimented.

## 2. Mechanical characterization of intracellular drug transport

### 2.1. Overview of optimization of chemical engineering principles

#### 2.1.1. Definitions and objectives

Optimization of chemical engineering principles refers to the process of finding the best parameters and conditions to improve production efficiency and economic benefits, reduce energy consumption and environmental pollution under the premise of ensuring the quality and safety of drugs [22,23]. It is a scientific method based on data, models and algorithms, aiming to find the optimal or near-optimal chemical engineering optimization scheme through the steps of experimental design, data analysis, model building, parameter optimization, and scheme evaluation. The goal of chemical engineering principal optimization is to make the production process reach the optimal or near-optimal in the following aspects under the premise of meeting the drug quality standards and safety norms: Maximize the transmission mechanical properties, purity, stability and bioavailability. Minimize by-products, waste, energy consumption and production costs. Optimization of production scale, equipment conditions, ease of operation and controllability. Optimal compliance with environmental protection requirements, social responsibility and market demands.

#### 2.1.2. Importance and areas of application

Optimization of chemical engineering principles is of key importance in pharmaceutical engineering. It not only improves drug quality and performance,

reduces cost and resource consumption, and enhances innovation and competitiveness, but also helps to enhance the protection of the environment and human health. The combined benefits of these aspects make chemical engineering principal optimization an indispensable core strategy in the pharmaceutical field, which promotes the continuous progress and sustainable development of drug R&D and production. Optimization of chemical engineering principles has a wide range of applications in chemical-pharmaceutical engineering, including drug synthesis, separation and purification, and formulation processes. In drug synthesis, optimizing reaction conditions and routes improves mechanical properties, transport efficiency, and reduces cost and energy consumption. In drug separation and purification, the optimal separation method is searched to improve efficiency and purity, and reduce loss and pollution. In drug formulation, chemical engineering principles optimization can improve the quality, performance and stability of the preparation, enhance drug absorption and bioavailability. Taken together, chemical engineering principles optimization promotes innovation and efficiency in the pharmaceutical field and is important for drug development and production.

#### 2.1.3. Optimization process

The chemical engineering principles optimization process is specifically based on mathematical models and algorithms to find the optimal or near-optimal solution through the steps of experimental design, data analysis, model building, parameter optimization, and solution evaluation. Chemical Engineering Principles Optimization is a critical engineering process that improves and optimizes drug cells through a series of steps to achieve higher quality, efficiency, and mechanical properties. Experimentation, data analysis, modeling, and optimization techniques are combined to achieve a drug cell delivery process with optimal mechanical properties.

### 2.2. Measurement of cellular mechanical properties and their optimization

#### 2.2.1. Measurement of cellular mechanical properties

At present, with the development of micro-nano manipulation, microfluidic chip, MEMS and other technologies, a series of effective methods for measuring the mechanical properties of cells have emerged, which can be categorized into two main groups according to whether or not they are in direct contact with the cells: contact and non-contact [24–26]. Contact measurement methods mainly include atomic force microscopy, parallel plate technique, squeeze deformation cytometry and microtubule aspiration, etc. Non-contact measurement methods mainly include magnetic tweezers, optical stretching, optical tweezers, shear and stretch flow deformation cytometry, dielectrophoretic stretching and acoustic methods, etc. Since this paper investigates, the mechanical properties of drug intracellular transport, optical tweezers technology in non-contact measurement methods is used to explore the mechanical properties of drug intracellular transport.

Optical tweezers technology is formed by a highly focused laser beam that captures particles through the gradient force generated by the interaction of the light intensity generated near the focal point with the particles themselves, the structure of the optical tweezers technology is shown in **Figure 1**. Polystyrene or silica

microspheres are generally attached to the surface of the cell, and the cell is manipulated by manipulating the captured microspheres, or the elastic modulus of the cell can be measured by indenting the cell by the force exerted on it by the captured microspheres. Optical tweezers are a non-contact method for accurately and non-destructively applying forces on the order of pico-Newtonian on the surface of a living cell, as well as contactless controlling the entire cell, or directly measuring forces acting in the cell membrane or cytoplasm.

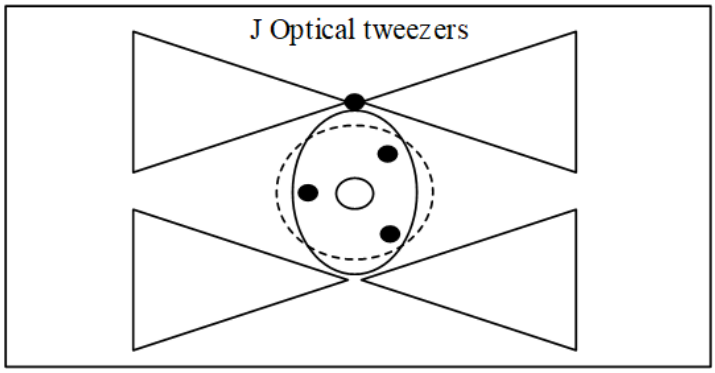


**Figure 1.** Optical tweezers technical structure.

Optical tweezers technology applies attractive or repulsive forces to microbeads or cells by means of light intensity gradient forces generated by a focused laser, and based on its mechanical model, it realizes high-precision measurements of very small cell-oriented forces (102 ~ 103 pN), and is able to directly measure forces acting on cell membranes or cytoplasm and study the viscoelasticity properties of cells. However, the force that can be applied by optical tweezers is limited, and is often used to study softer cells, such as red blood cells. Meanwhile, the traditional optical tweezers technique also faces the problems of cumbersome operation procedures and low throughput when measuring the mechanical properties of cells. On the one hand, optical tweezers can be used to replace manual labor by combining with automation technology to improve the measurement efficiency. On the other hand, it can be combined with microfluidics and other technologies to realize the standardization and automation of the operation procedure, so as to achieve high-precision and high-throughput measurements of individual cells and even organelles, and the measurement of intracellular transport of drug cell mechanical properties is also a field to be explored, which can enable people to comprehensively understand the state of the cells, thus promoting the pre-diagnosis of diseases.

### 2.2.2. Optimization of cell mechanical properties

Currently, most of the applications based on the mechanical properties of cells use model building to realize the determination and identification of abnormal cells, so as to realize the diagnosis of diseases and other applications. These traditional methods rely on the theoretical research ability of researchers and a large amount of labor, which is less efficient.

The combination of artificial intelligence and cellular mechanical properties is not only a novel way to classify mixed cell populations, but also faster and more successful, which could also improve the overall success rate of cell-based therapies.

Therefore, in the future, more, smarter and more powerful AI methods can be designed to provide technical support for more applications, such as rare cell discovery and sorting based on cellular mechanical properties, and intelligent diagnosis of diseases, with a view to improving efficiency and success rates.

The research on cellular mechanical properties of intracellular transport of drugs has been optimized and improved in terms of high-throughput, standardized and multi-parameter measurements, and new methods have been proposed, which will be helpful for people to more comprehensively and accurately achieve the characterization of the mechanical properties of cells and the elucidation of the state of microphysiology and pathology, and it will also help to improve the efficiency and accuracy of the diagnosis of diseases, and help to rapidly and accurately develop and test novel drugs from the cellular level, which will provide new support to the development of medical and health care. The research will also help to improve the efficiency and accuracy of disease diagnosis and the rapid and accurate development and testing of novel drugs at the cellular level, thus providing a new boost to the development of healthcare.

## 2.3. Cell mechanics optimization model

The cellular mechanical properties of drug intracellular transport mainly involve the forces between the cell and the drug carrier, and between the cell and the substrate, which combine to accomplish various physiological functions of the cell. Various mechanical scenarios encountered by drug cells during transport, such as torsion, elongation, extrusion, shear, etc., are simulated. By simulating these mechanical effects, the displacements and deformations generated between cells and cells and drug carriers, and between cells and substrates can be studied. The viscoelasticity model is widely recognized to be useful for describing the mechanical properties of drug intracellularly transported cells; this model has only three parameters, each of which has a clear physical meaning. This simplicity and clarity make this model more favorable to researchers. How to find the viscoelasticity three parameters that characterize the mechanical properties of drug intracellular transport? We adopted the optimization method commonly used in chemical engineering principles, by constantly changing the parameters of drug intracellular transport cells and setting up certain criteria, we optimized to get the parameters that best represent the mechanical properties of drug intracellular transport cells.

### 2.3.1. Overview of optimization methods based on parameter separation

The influence of each of the three parameters of cellular viscoelasticity on its mechanical response is understood both theoretically and numerically. Where, $k_1$ is known as the equilibrium modulus of a viscoelastic material, which determines the mechanical response of a viscoelastic material when it reaches equilibrium under a constant load. $k_1 + k_2$ is called the transient modulus of the viscoelastic material, which is the elastic modulus at the moment of initial response to the load. The viscous coefficients $\eta$ and $k_2$ together determine the characteristic time of the mechanical response of a viscoelastic material, which portrays the rate of evolution of the viscoelastic material from the onset of the initial deformation to the entry into the final equilibrium state response. The three parameters of viscoelasticity can be separated and grouped into their specific problems, and these three parameters can be derived

one by one after analyzing the specific problems separately ($k_1$, $k_2$, $\eta$). First, since the response of the drug cell at equilibrium is only determined by the equilibrium modulus $k_1$, the response of the drug cell after reaching equilibrium can be analyzed in an attempt to find an optimal value of $k_1$ that would allow the drug cell configuration calculated by the model at equilibrium to match the experimentally measured drug cell configuration. Second, since the initial response of the drug cell to the load is determined by the instantaneous modulus $k_1 + k_2$, based on the optimized solution of $k_1$ obtained in the first step, it is now sufficient to try to find the optimized value of $k_2$ so that the drug cell configuration calculated by the model at the moment of the initial response coincides with the experimentally measured drug cell configuration. Finally, we have optimized the values of $k_1$ and $k_2$, leaving only the viscosity coefficient $\eta$ to be found independently. While $\eta$ is the characteristic time of the mechanical response of a viscoelastic material together with $k_2$, if we know the relationship between $\eta$ and the characteristic time of the drug cell deformation under shear flow and can find this characteristic time, then the coefficient of viscosity $\eta$ can be defined naturally.

#### 2.3.2. Program implementation of the optimization algorithm

Conformational data of cells after actual deformation were obtained directly from experimental data based on optical tweezers technology. Subsequently, an objective function is defined to characterize the difference between the post-deformation configuration of the cells and the post-deformation configuration of the cells obtained through experiments. Finally, a reasonable convergence criterion for the conformational difference is set. If the value of the objective function satisfies this convergence criterion, the cell viscoelasticity parameters set in the drug cell transport mechanics model are considered as the final optimization results; if the value of the objective function does not satisfy this convergence criterion, the process values of the optimization parameters are adjusted according to the optimization speed curve, and the adjusted process values of the optimization parameters are returned to the drug cell transport mechanics model for the next iterative calculation. Return the adjusted optimized parameter values to the drug cell transport mechanics model and carry out the next iterative calculation until the adjusted cell viscoelasticity data can make the objective function satisfy the convergence condition.

## 3. Analysis of drug cell mechanics studies

### 3.1. Measurement of cell mechanical properties based on optical tweezers technology

#### 3.1.1. Cell sample preparation

Prepare 5 copies of co-cultivated drug cells and microspheres according to the drug cell and microsphere sample preparation method. $H_2O_2$ solution with a concentration of 30% was purchased, and four working solutions with concentrations of 80 $\mu M$, 160 $\mu M$, 240 $\mu M$ and 320 $\mu M$ were prepared with PBS buffer for use. The thickness of the glass-bottomed Petri dishes used for sample observation was 0.16 mm, and 1% bovine serum albumin was added before use to prevent cells or microspheres from adhering to the bottom of the Petri dish and affecting the manipulation of the

light trap. Add 100 $\mu L$ bovine serum albumin solution to the petri dish, place it in a biological safety cabinet, and wait for the solution to evaporate completely to complete the closure.

Five samples of cells and microspheres were taken, and the supernatant after centrifugation was removed and resuspended by adding 2 ml of PBS and four $H_2O_2$ solutions at concentrations of 80 $\mu M$, 160 $\mu M$, 240 $\mu M$, and 320 $\mu M$, respectively. The five resuspended samples were added to five closed petri dishes and left at room temperature for 20 min for observation and measurement.

### 3.1.2. Optical tweezers procedure

The stiffness of the light trap was first calibrated before the measurements began. Observe the petri dish under a microscope using a 60× oil immersion objective to find a freely suspended microsphere and capture it using the light trap. It is sufficient to record a video of this microsphere containing approximately 6000 images. The trajectory of the microsphere's thermal noise motion around the center of the light trap is analyzed to derive a probability distribution curve for the displacement of the microsphere, which is then combined with the Boltzmann distribution to calculate the light trap stiffness. After the calibration of the light trap stiffness was completed, drug cells meeting the requirements for dual light trap manipulation, i.e., one microsphere adhered to each side of the level of a blood drug cell, were found in the petri dish. Two light traps with consistent parameters were set up to capture two microspheres on each side of the drug cell. During the manipulation process, one light trap was kept stationary and a motion sequence was added to the other light trap so that the light trap maintained a uniform lateral horizontal motion of 50 nm/s to stretch the drug cell and record a series of hologram images during the process. As before, in order to exclude errors introduced by differences in drug cell size, 10 of the compliant drug cells in each sample were randomly selected for measurement.

Compared with other micromanipulation techniques, optical forceps have the following three advantages to show their performance in the field of biological measurement:

(1) High resolution, up to subcutaneous magnitude, very suitable for biomechanical property measurement.

(2) The manipulation of biological objects is non-invasive, which can reduce the interference of instruments on biological objects in biological research.

(3) Simple structure, easy to build, mainly through the optical lens to converge the laser to a point to form optical tweezers, according to demand can be free to add other devices or combine other technologies to achieve different functions.

### 3.1.3. Analysis of results

**Figure 2** illustrates the thickness images derived from the recovery of one compliant hemoglobin drug cell from each of the five groups of samples. **Figure 2a**,**b**–**e** show images of drug cell thickness changes in PBS and in $H_2O_2$ solutions at concentrations of 80 $\mu M$–320 $\mu M$, respectively, with four pairs of images in each group corresponding to changes in light trapping power from 0 to 3 pN. In order to emphasize the variation of the maximum drug cell thickness, only the data for the drug cell thickness range above 2 $\mu m$ are shown in the figure. From the four sets of images in **Figure 2a**, it can be seen that the thickness of normal hemoglobin drug cells in PBS

subjected to the light trap pulling force changes more significantly, while the changes in drug cell thickness become weaker and weaker with the increase of oxidative stress in the series of images in **Figures 2b**–**e**. In particular, the thickness of drug cells subjected to double light trap stretch in **Figure 2e** hardly changed. These measurements reflect the deterioration of the deformation ability of the drug cell after oxidative stress, which reflects the trend of the elastic modulus of the drug cell becoming smaller.

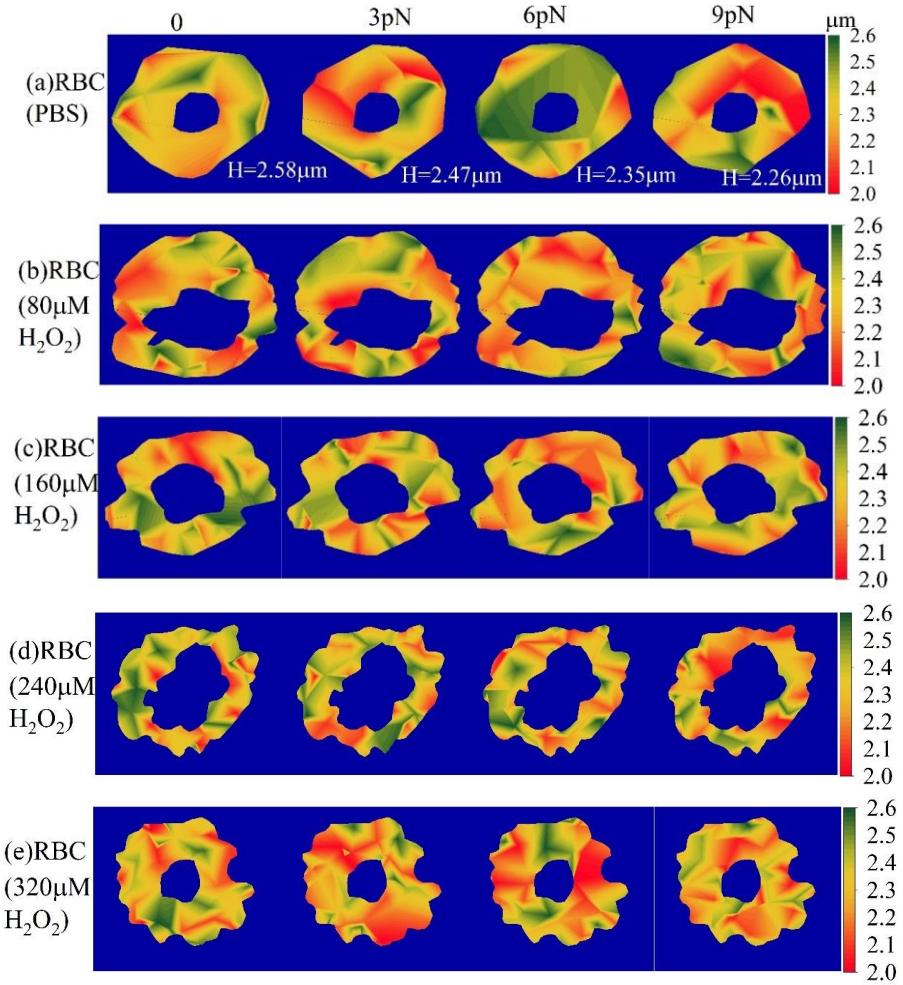


**Figure 2.** Hemoglobin drug cell thickness image. **(a)** RBC (PBS); **(b)** RBC (80μM $H_2O_2$); **(c)** RBC (160μM $H_2O_2$); **(d)** RBC (240μM $H_2O_2$); **(e)** RBC (320μM $H_2O_2$).

**Figure 3** shows the average value of the axial maximum height change rate of 10 cells taken from each of the 5 sets of samples versus the corresponding light trap stretching force. It can be seen that during the variation of the light trap force from 0 to 9 pN, the cell thicknesses all decrease with stretching as the cells are stretched laterally. Comparing the slopes of the fitted curves of the thickness of normal drug cells in PBS as a function of the light trap force, the slopes of the curves of the thickness of drug cells subjected to oxidative stress as a function of the light trap force decreased significantly, and the larger the concentration of the $H_2O_2$ solution, the smaller the slopes. This indicated that the structural composition of the cell membrane was changed after the drug cells were subjected to oxidative stress during transport,

and the deformation ability of the cells became worse, which also verified that oxidative stress would lead to the elastic modulus of the drug cell membrane becoming smaller.

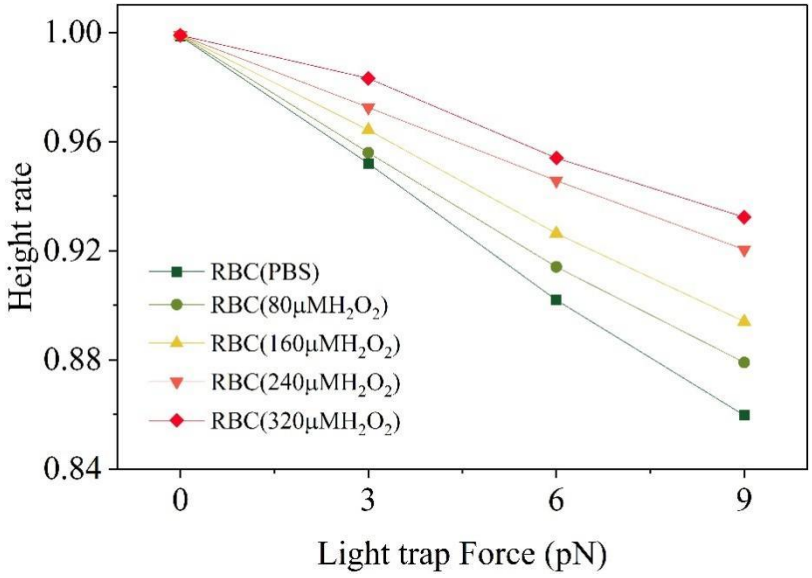


**Figure 3.** Relationship between thickness change rate and tension of optical trap.

By solving the drug cell thickness, the volume of the whole drug cell, i.e. drug cell volume, can be calculated from the thickness values of different parts of the drug cell. Drug cell volume is another important indicator of the state of drug cells, and the volume of blood cells often changes along with the abnormal condition of the cells. **Table 1** shows the comparison of the mean values of drug cell volume in five groups of samples. It can be seen from the data in the table that the average volume of normal drug cells in PBS is 88.37 fL, which is within the normal value range of 86–100 fL. As the concentration of H2O2 solution increased, the mean volume of drug cells decreased significantly.80 $\mu M$–320 $\mu M$ the mean volume of drug cells in hydrogen peroxide solution decreased to 80.62 fL, 80.14 fL, 78.73 fL and 77.78 fL, respectively.

**Table 1.** Comparison of mean cell volume.

| Sample | Volume (fL) |
|---|---|
| RBC (PBS) | 88.37 |
| RBC (80 $\mu M$ $H_2O_2$) | 80.62 |
| RBC (160 $\mu M$ $H_2O_2$) | 80.14 |
| RBC (240 $\mu M$ $H_2O_2$) | 78.73 |
| RBC (320 $\mu M$ $H_2O_2$) | 77.78 |

The change of drug cell morphology with time during the recovery of the original appearance after the force was calculated, and **Figure 4** shows the comparison of axial heights of the cell after deformation by uniaxial tensile force to the disappearance of the tensile force and the recovery of the cell to its original appearance, in which **Figure 4a**,**b** are before and after the recovery, respectively. The effect of oxidative stress on the recovery ability of cell morphology can be obtained by making the above

observations on normal state hemoglobin cells and hemoglobin cells subjected to different degrees of oxidative stress. Again, in order to exclude the error caused by the different cell sizes, 10 randomly selected cells in each sample that met the requirements were still measured and averaged.

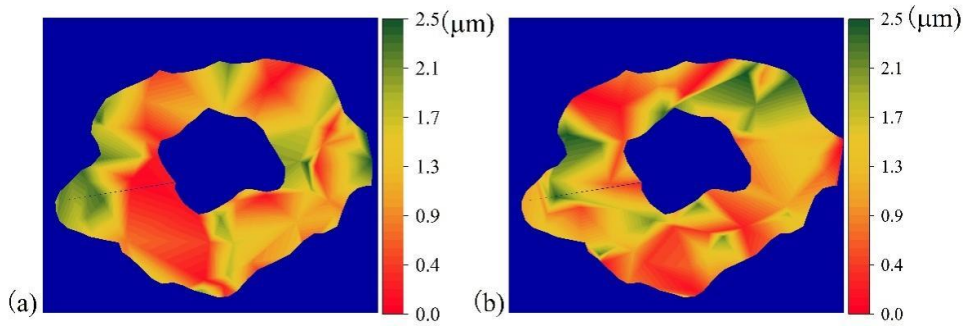


**Figure 4.** Axial height comparison of deformation to restore original appearance. **(a)** Before recovery; **(b)** After recovery.

In order to facilitate the comparison of the axial height change rate with time during the recovery process of different groups of drug cells, data with height change rate H/H0 in the range of 090 to 1 were uniformly selected for observation. **Figure 5** shows the average rate of height change versus time for normal drug cells placed in PBS and drug cells placed in different concentrations of hydrogen peroxide solution. It can be seen from the figure that the rate of recovery of all five groups of cells in the process of morphological recovery becomes gradually faster with time. Comparing the recovery rate of normal drug cells in PBS, the drug cells stimulated by hydrogen peroxide recovered faster. As the concentration of hydrogen peroxide solution increased, the time required for the drug cells to recover their original appearance became shorter. This experiment again verified that the elastic modulus of the drug cell membrane becomes larger with the increase of the degree of oxidative stress, i.e., the stiffness of the cell membrane becomes larger and the deformation ability of the drug cell becomes worse. In summary, it was verified that the mechanical properties of the drug measured by the above operation procedure were in line with the reality, which laid the foundation for the subsequent experimental study of cell microdeformation measurement.

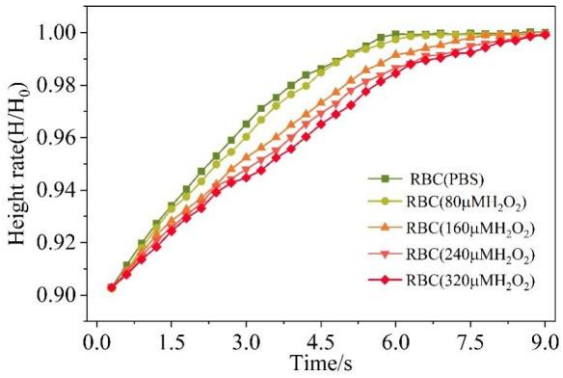


**Figure 5.** The relationship between the rate of change from height to height and time.

## 3.2. Cell mechanics optimization model validation analysis

### 3.2.1. Analysis of optimization results

The minimum deformation curves optimized by parameters $k_1$, $k_2$, and $\eta$ for different transport times are given in **Figure 6**, where the horizontal axis is the transport time and the vertical axis is the transport time. Regardless of the parameters $k_1$, $k_2$ and $\eta$, the longer the transportation time, the larger the deformation of drug cells will be. Moreover, the deformation of drug cells when reaching the predefined elastic force is small when transporting with the transport speed curve optimized by parameter $\eta$, while the transport speed is the largest, and the deformation obtained with the transport speed curve of parameter $k_2$ is in between. It can be seen that the transport speed profile in the form of viscoelasticity parameter optimization can effectively reduce the deformation of the cells during transport, and the degree of reduction increases with the reduction of transport time.

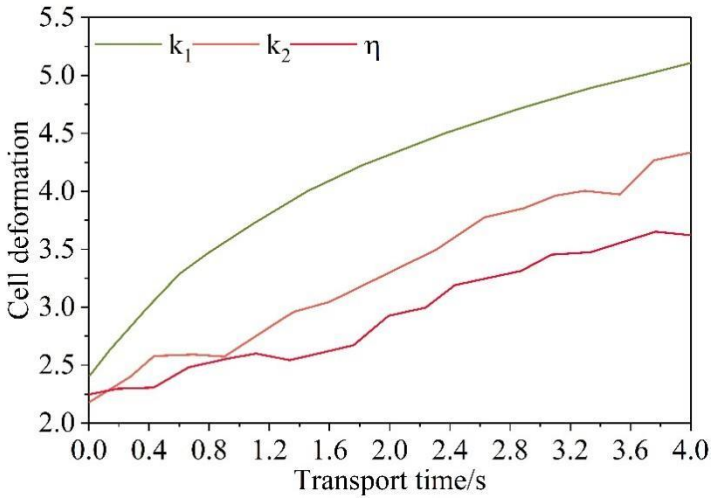


**Figure 6.** Minimum deformation curve.

### 3.2.2. Experimental validation

The algorithmic process of viscoelasticity parameter optimization is based on the following assumptions: (1) an accurate cell force deformation model, (2) the drive system can precisely execute the action in accordance with the velocity profile of the viscoelasticity parameter, and (3) the cell will rupture when the set contact force size is reached. In fact, although these three assumptions are difficult to satisfy in practical applications, optimization to derive the viscoelasticity parameters is still of practical value. In this section, experiments are designed to demonstrate the validity of the above optimized viscoelasticity parameter curves derived from theoretical calculations.

Because the contact force reaches the predetermined contact force at the moment t is an important nonlinear equation constraint in the optimization problem, and its constraint strength is large, and in fact the contact force reached by each drug cell transport is also different, so in the actual operation process can be adjusted to the optimized viscoelasticity parameter velocity curve as follows: if the contact force does not reach the predetermined value at the time of reaching the moment *t*, or the drug If the contact force does not reach the preset value at the moment *t*, or the drug cell does

not start to transport, let the transport speed remain at the value of the moment t to continue the transportation activity.

Using the viscoelasticity parameters optimized in **Figure 6** to investigate the mechanical properties of a drug cell transport experiments, transport time *t* selected as {0.4, 0.8, 1.2, 2.2, 2.8, 3.4, 4}, in addition to selecting four constant viscoelasticity parameters of the speed of the most control, respectively, for the 0.8 mm/s, 1.2 mm/s, 2 mm/s and 3 mm/s, set the drug cell The contact force is 800 $\mu N$, which can be converted to the constant speed corresponding to the transportation time consumed is divided into {2.162, 1.643, 0.4681, 0.297}, the experimental results of the drug cell transportation deformation is shown in **Figure 7**. The experimental results show that the optimized viscoelasticity parameter speed curve for transportation, the deformation of drug cells is between 430 um and 690 um, generally lower than the deformation of drug cells under the constant speed transportation, and the deformation can be as small as 423 um. It can be seen that the optimized viscoelasticity parameter speed curve can effectively reduce the mechanical damage of the drug cells in the transportation process.

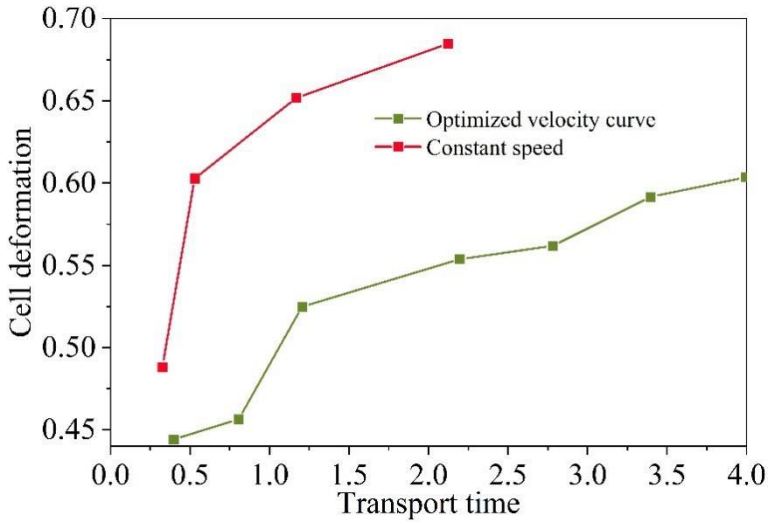


**Figure 7.** Experimental results of drug cell transport deformation.

## 3.3. Pharmacodynamic assessment based on cellular mechanical characterization assays

Mechanical properties of cells can effectively characterize the physiological state of cells and can be used as a label-free covariate for detecting cell status, metastatic potential and degree of differentiation for the study, diagnosis and treatment of diseases. In this subsection, drug sensitivity studies of cells were performed using an anticancer drug (enzalutamide) on the basis of cell mechanical characterization. By comparatively analyzing the changes in the mechanical properties of PC-3 cells (androgen non-sensitive) and LNCaP (androgen-sensitive) cells treated with different anticancer drugs, the differences in the drug sensitivity of the cells and the effects of the different drugs on the cells were evaluated, which proved that the application of the cellular mechanical properties assay based on optical tweezers technology is promising for the assessment of drug efficacy and drug screening.

In this subsection, the drug enzalutamide, an androgen receptor antagonist, was used as an example to inhibit the proliferation of prostate cancer cells by inhibiting the binding of androgens to prostate cancer cells. To further understand the effects of different concentrations of enzalutamide on the mechanical properties of androgen non-sensitive prostate cancer cells PC-3 and androgen-sensitive prostate cancer cells LNCaP, the two types of cells were cultured using configured complete medium containing 5 nmol/L, 50 nmol/L, 500 nmol/L, and 5000 nmol/L concentrations of enzalutamide, respectively. In order to visually compare the effects of enzalutamide on PC-3 cells and LNCaP cells, the area and deformation of the cells were detected using light tweezers technique and compared with the untreated control group The changes in the area and deformation of the two types of cells under different concentrations of the drug were statistically analyzed, and the analysis of the area and deformation of the cells under different concentrations is shown in **Figure 8**, where **Figure 8a**,**b** denote area and deformation. The results showed that there was no significant change in the area and deformation of PC-3 cells under different concentrations of enzalutamide, while the LNCaP cells showed changes in cell area and deformation, but to a lesser extent, and the mean value of the area and the mean value of the deformation of the LNCaP cells were minimized when the concentration of enzalutamide was 1000 nM, which were 175.4$\mu m^2$ and 0.048$\mu m$, respectively.

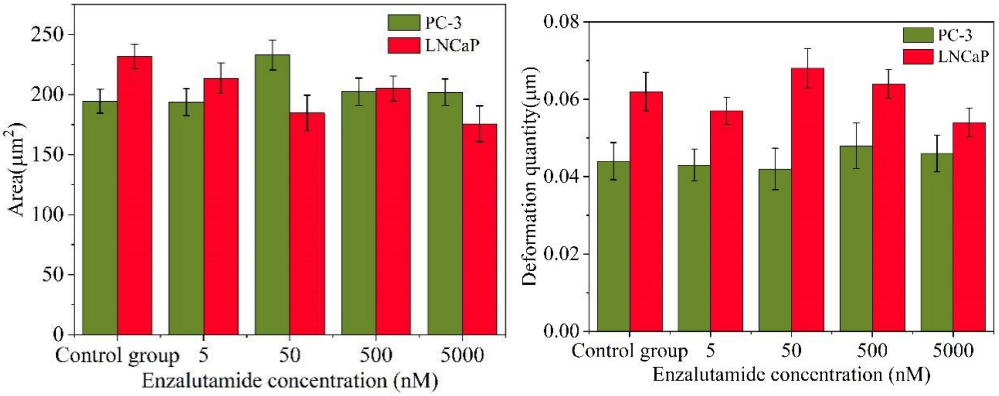


**(a)** **(b)**

**Figure 8.** Cell area and deformation analysis at different concentrations. **(a)** area; **(b)** deformation quantity.

To further investigate the trend of the two types of cells in enzalutamide, a comparison of the 50% density contours of the two types of cells is shown in **Figure 9**, where **Figure 9a**,**b** are PC-3 and LNCaP, respectively. androgen non-sensitive prostate cancer cells PC-3 did not show any significant changes in cell area and cell morphology after incubation with different concentrations of enzalutamide for 24 h, whereas androgen-sensitive prostate cancer cells LNCaP showed no significant changes in cell area and cell morphology, whereas androgen-sensitive prostate cancer cells LNCaP showed significant changes in cell area and cell morphology in relation to enzalutamide concentration. Because enzalutamide is an androgen antagonist that inhibits the binding of androgens to their receptors, and PC-3 cells are not sensitive to androgens, enzalutamide does not affect the morphology and growth of PC-3 cells in terms of the mechanism of drug action. In contrast, LNCaP, as androgen-sensitive

prostate cancer cells, the cell area and deformation under the action of enzalutamide gradually decreased with the increase of drug concentration. This was also demonstrated by the experimental results in **Figure 9**. The changes in area and deformation of LNCaP cells under different concentrations of enzalutamide after 24 h of culture were not as obvious as those under docetaxel, which demonstrated that the change of mechanical properties of cells by enzalutamide is a slow process, and it needs a longer incubation time to see a more obvious difference. Combined with the is viscoelastic line, and taking into account the trend of area and shape variables of PC-3 cells and LNCaP cells, the mechanical properties of prostate cancer cell line PC-3 were not altered under the action of enzalutamide. With increasing enzalutamide concentration, the hardness of LNCaP cells increased at low drug concentrations (5 nmol/L, 50 nmol/L) and gradually decreased at high drug concentrations (500 nmol/L, 5000 nmol/L) as the cells adapted to the effects of the drug. This reflects the gradual conversion of androgen-sensitive prostate cancer LNCaP cells to androgen-independent in order to adapt to the androgen-deficient environment under the effect of enzalutamide. Overall, the stiffness of PC-3 cells did not change under the effect of enzalutamide, while LNCaP hardened, successfully validating the efficacy of the cellular mechanical characterization-based assessment of drug efficacy.

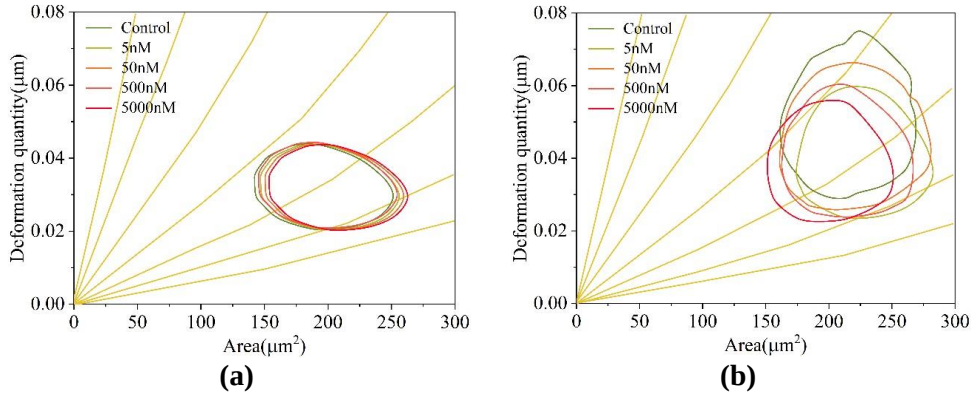


**Figure 9.** Comparison of 50% density contour lines between the two cells. **(a)** PC-3; **(b)** LNCaP.

## 4. Conclusion

In the article, drug cell pharmaceutical samples were produced, their mechanical properties were measured with the help of optical tweezers technology, and a cellular mechanical optimization model based on viscoelasticity three parameters was constructed. The mechanical properties of drug cell transport were investigated using experimental validation analysis. The average volume of normal drug cells in PBS was 90 fL, which was within the normal value range of 86–100 fL. As the concentration of $H_2O_2$ solution increased, the average volume of drug cells decreased significantly, resulting in the elastic modulus of the drug cell membrane becoming larger with the increase in the degree of oxidative stress, the stiffness of the cell membrane becoming larger, and the deformation ability of the drug cell becoming poorer, which indicated that the mechanical properties of the drug measured in accordance with the above procedure were in line with reality. After optimization, the deformation of drug cells was all between 430 um and 690 um, which was smaller than that of drug cells under

constant velocity transport, indicating that the optimized velocity profile of viscoelasticity parameter was able to alleviate the mechanical damages produced by drug cells in the transport process. The trend of deformation variables, prostate cancer cell line PC-3 did not change the mechanical properties under the effect of drug. The hardness of LNCaP cells was positively correlated with low drug concentration (5 nmol/L, 50 nmol/L), when in high drug concentration (500 nmol/L, 5000 nmol/L) on the contrary, it showed a negative correlation. This indicates that PC-3 cells did not show any changes under the effect of enzalutamide, while LNCaP was able to observe significant changes, which explains the mechanical properties of the drug intracellularly in a comprehensive manner.

Optical tweezers technology is the intersection of two basic disciplines of physics and biology, which provides an excellent point for the combination of new experimental techniques and methods with major basic biological problems, and has played an important role in the research of several basic problems in life science. As a forward-looking basic research direction, it is also bound to produce a variety of practical technologies and methods, and will have a broad development prospect. As a nanodisplacement manipulation method and a probe of the small interaction force between particles (pN order), it is not only used in the field of life science, but also suitable for other research and application fields involving small particles.

There are still some problems to be studied and improved in this paper. The next step is as follows:

(1) The influence of the numerical aperture of the optical tweezers on the maximum transverse filtering force of the particles was theoretically analyzed.

(2) Further develop the measurement system to make its operation simpler and the measurement results more accurate, and use this system to measure the surface charge of biological cells such as red blood cells.

**Ethical approval:** Not applicable.

**Conflict of interest:** The author declares no conflict of interest.

## References

1. Ruan, S., Zhou, Y., Jiang, X., & Gao, H. (2021). Rethinking CRITID procedure of brain targeting drug delivery: circulation, blood brain barrier recognition, intracellular transport, diseased cell targeting, internalization, and drug release. Advanced Science, 8(9), 2004025.
2. Hinde, E., Thammasiraphop, K., Duong, H. T., Yeow, J., Karagoz, B., Boyer, C., ... & Gaus, K. (2017). Pair correlation microscopy reveals the role of nanoparticle shape in intracellular transport and site of drug release. Nature Nanotechnology, 12(1), 81-89.
3. Zhang, J., Liu, D., Zhang, M., Sun, Y., Zhang, X., Guan, G., ... & Hu, H. (2016). The cellular uptake mechanism, intracellular transportation, and exocytosis of polyamidoamine dendrimers in multidrug-resistant breast cancer cells. International journal of nanomedicine, 3677-3690.
4. Harisa, G. I., & Faris, T. M. (2019). Direct drug targeting into intracellular compartments: issues, limitations, and future outlook. The Journal of Membrane Biology, 252(6), 527-539.
5. Mateus, A., Treyer, A., Wegler, C., Karlgren, M., Matsson, P., & Artursson, P. (2017). Intracellular drug bioavailability: a new predictor of system dependent drug disposition. Scientific reports, 7(1), 43047.

6. Lei, B., Zhang, Y., Chen, M., Xu, S., & Liu, H. (2022). Intracellular transport of biomacromolecular drugs by a designed microgel capsule with pH/redox stimulus-responsiveness. Colloids and Surfaces A: Physicochemical and Engineering Aspects, 648, 129269.
7. Lv, C., Yang, C., Ding, D., Sun, Y., Wang, R., Han, D., & Tan, W. (2019). Endocytic pathways and intracellular transport of aptamer-drug conjugates in live cells monitored by single-particle tracking. Analytical chemistry, 91(21), 13818-13823.
8. He, S., Singh, D., & Helfield, B. (2022). An overview of cell membrane perforation and resealing mechanisms for localized drug delivery. Pharmaceutics, 14(4), 886.
9. Du, X., Wang, J., Zhou, Q., Zhang, L., Wang, S., Zhang, Z., & Yao, C. (2018). Advanced physical techniques for gene delivery based on membrane perforation. Drug delivery, 25(1), 1516-1525.
10. Stewart, M. P., Langer, R., & Jensen, K. F. (2018). Intracellular delivery by membrane disruption: mechanisms, strategies, and concepts. Chemical reviews, 118(16), 7409-7531.
11. Mathiyazhakan, M., Wiraja, C., & Xu, C. (2018). A concise review of gold nanoparticles-based photo-responsive liposomes for controlled drug delivery. Nano-micro letters, 10, 1-10.
12. Ding, H., Tan, P., Fu, S., Tian, X., Zhang, H., Ma, X., ... & Luo, K. (2022). Preparation and application of pH-responsive drug delivery systems. Journal of Controlled Release, 348, 206-238.
13. Sung, Y. K., & Kim, S. W. (2020). Recent advances in polymeric drug delivery systems. Biomaterials Research, 24(1), 12.
14. Dong, X. (2018). Current strategies for brain drug delivery. Theranostics, 8(6), 1481.
15. Rai, M. F., & Pham, C. T. (2018). Intra-articular drug delivery systems for joint diseases. Current opinion in pharmacology, 40, 67-73.
16. Haley, R. M., Gottardi, R., Langer, R., & Mitchell, M. J. (2020). Cyclodextrins in drug delivery: applications in gene and combination therapy. Drug delivery and translational research, 10, 661-677.
17. Peynshaert, K., Devoldere, J., De Smedt, S. C., & Remaut, K. (2018). In vitro and ex vivo models to study drug delivery barriers in the posterior segment of the eye. Advanced drug delivery reviews, 126, 44-57.
18. Czapar, A. E., & Steinmetz, N. F. (2017). Plant viruses and bacteriophages for drug delivery in medicine and biotechnology. Current opinion in chemical biology, 38, 108-116.
19. Degors, I. M., Wang, C., Rehman, Z. U., & Zuhorn, I. S. (2019). Carriers break barriers in drug delivery: endocytosis and endosomal escape of gene delivery vectors. Accounts of chemical research, 52(7), 1750-1760.
20. Parodi, A., Molinaro, R., Sushnitha, M., Evangelopoulos, M., Martinez, J. O., Arrighetti, N., ... & Tasciotti, E. (2017). Bio-inspired engineering of cell-and virus-like nanoparticles for drug delivery. Biomaterials, 147, 155-168.
21. Ren, S., Wang, M., Wang, C., Wang, Y., Sun, C., Zeng, Z., ... & Zhao, X. (2021). Application of non-viral vectors in drug delivery and gene therapy. Polymers, 13(19), 3307.
22. Xiaolong Li,Danhui Gao,Junlei Tang,Ruixiao Lin,Hang Li,Ruomei Qi... & Wenying Li. (2024). Optimization of chemical engineering control for large-scale alkaline electrolysis systems based on renewable energy sources. International Journal of Hydrogen Energy193-206.
23. Ashley Pennington. (2024). From A PhD in Chemical Engineering to a Career in Science Policy. Chemical Engineering Progress(10),28-32.
24. Yu Yan,Tiean Zhou,Yu Zhang,Zhicheng Kong,Weisong Pan & Chengfang Tan. (2024). Comparing the Mechanical Properties of Rice Cells and Protoplasts under PEG6000 Drought Stress Using Double Resonator Piezoelectric Cytometry. Biosensors(6),
25. Weber Andreas,Benitez Rafael & TocaHerrera José L. (2022). Measuring (biological) materials mechanics with atomic force microscopy. 4. Determination of viscoelastic cell properties from stress relaxation experiments. Microscopy research and technique(10),3284-3295.
26. Kendra D. Nyberg,Kenneth H. Hu,Sara H. Kleinman,Damir B. Khismatullin,Manish J. Butte & Amy C. Rowat. (2017). Quantitative Deformability Cytometry: Rapid, Calibrated Measurements of Cell Mechanical Properties. Biophysical Journal(7),1574-1584.